



**Shape Control of Mesoporous Silica Nanomaterials  
Templated with Dual Cationic Surfactants and Their  
Antibacterial Activities**

Journal:	<i>Biomaterials Science</i>
Manuscript ID:	BM-COM-06-2015-000197.R1
Article Type:	Communication
Date Submitted by the Author:	04-Aug-2015
Complete List of Authors:	Hao, Nanjing; University of Massachusetts Lowell, Chen, Xuan; University of Massachusetts Lowell, Chemistry Jayawardana, Kalana; University of Massachusetts Lowell, Chemistry Wu, Bin; University of Massachusetts Lowell, Chemistry Sundhoro, Madanodaya; University of Massachusetts Lowell, Chemistry Yan, Mingdi; University of Massachusetts Lowell, Chemistry

## Shape Control of Mesoporous Silica Nanomaterials Templated with Dual Cationic Surfactants and Their Antibacterial Activities

Cite this: DOI: 10.1039/x0xx00000x

Received 00th January 2012,  
Accepted 00th January 2012

Nanjing Hao, Xuan Chen, Kalana W. Jayawardana, Bin Wu, Madanodaya Sundhoro and Mingdi Yan\*

DOI: 10.1039/x0xx00000x

www.rsc.org/

**Mesoporous silica nanomaterials of different shapes (film, platelet, sphere, rod) were synthesized simply by tuning the mole ratio of dual cationic surfactant templates, cetyltrimethylammonium bromide (CTAB) and tetrabutylammonium iodine (TBAI). The film showed the most potent antibacterial activities against mycobacteria.**

Mesoporous silica nanomaterials (MSNs) have shown a wide range of potential applications in drug delivery,<sup>1</sup> protein transportation,<sup>2</sup> bioimaging,<sup>3</sup> cancer therapy,<sup>4</sup> catalysis,<sup>5</sup> renewable energy,<sup>6</sup> and biosensing.<sup>7</sup> MSNs are generally prepared from alkoxysilanes or silicates using a base or acid catalyst, and an organic surfactant or a block copolymer as the structure-directing template.<sup>8</sup> Recent work have shown that the particle shape plays a critical role in successfully realizing many of the aforementioned applications.<sup>9</sup>

In this context, much effort has been devoted to the synthesis of MSNs of different shapes. For example, MSNs of various aspect ratios from sphere to rod can be prepared by changing the concentration of cationic surfactant and/or catalyst,<sup>10</sup> the catalyst type,<sup>11</sup> stirring rate,<sup>12</sup> or introducing an anionic surfactant as co-template,<sup>13</sup> an organic solvent as co-solvent,<sup>14</sup> or an organoalkoxysilane as co-precursor.<sup>15</sup> However, shapes other than sphere or rod have not been reported following these general synthetic strategies. Mesoporous silica platelets and films are two mesoporous silica structures that have shown promises in separation, catalysis, and biomedical applications.<sup>16</sup> There are limited methods for the synthesis of well-defined mesoporous silica platelets.<sup>17</sup> One strategy is to use cationic/anionic surfactant as the confining bilayer and then let Pluronic123/silicate nanocomposite intercalate between the bilayers.<sup>17a</sup> Another strategy involved cocondensation of silicate and aminopropyltriethoxysilane in surfactant solution under strongly acidic and microwave irradiation conditions.<sup>17b</sup> Mesoporous silica films have been prepared by self-assembly at solid/liquid/vapor interfaces by dip-/spin- coating on solid substrate.<sup>18</sup> However, these strategies are relatively complex and tedious, and most importantly, difficult to alter particle shape. Herein, we report a general strategy to synthesize MSNs of various shapes, including film-, platelet-, sphere-, and rod- like MSNs, by simply tuning the mole ratio of dual cationic surfactant templates, cetyltrimethylammonium bromide (CTAB) and tetrabutylammonium iodine (TBAI). These MSNs were further tested against mycobacteria (*M. smegmatis* strain mc<sup>2</sup> 651) to study the role of particle shape on the antibacterial activity.

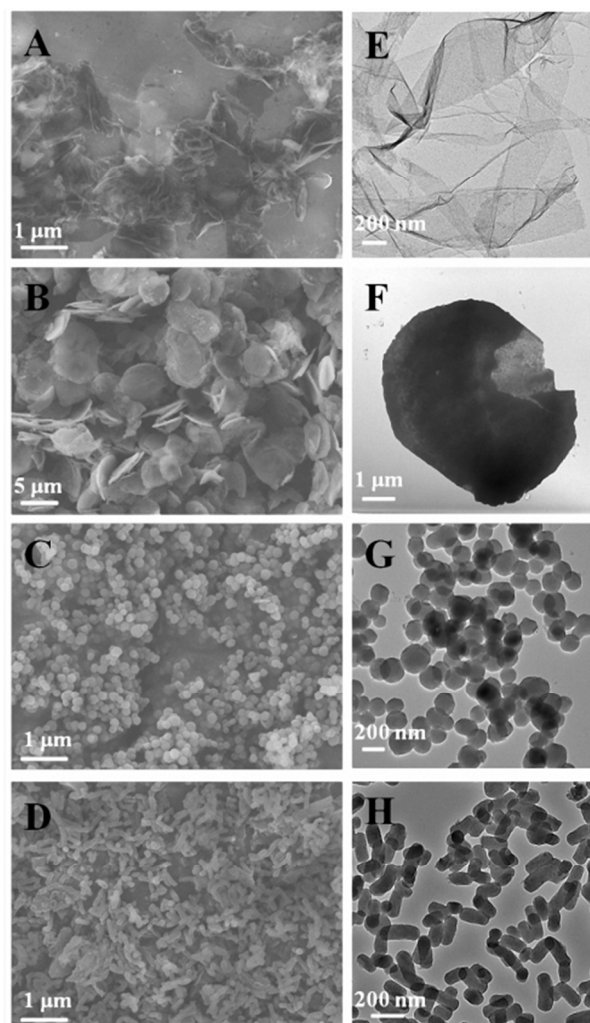


**Fig. 1** SEM and TEM images of as-synthesized mesoporous silica films (FMSN, R=0.8, A & E), platelets (PMSN, R=1.5, B & F), spheres (SMSN (R=2.5, C & G), rods (RMSN, R=4, D & H). R is the mole ratio of the two templates ([CTAB]/[TBAI]) used during the synthesis.

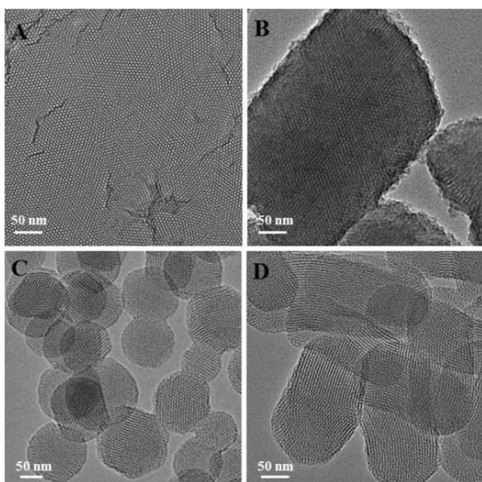
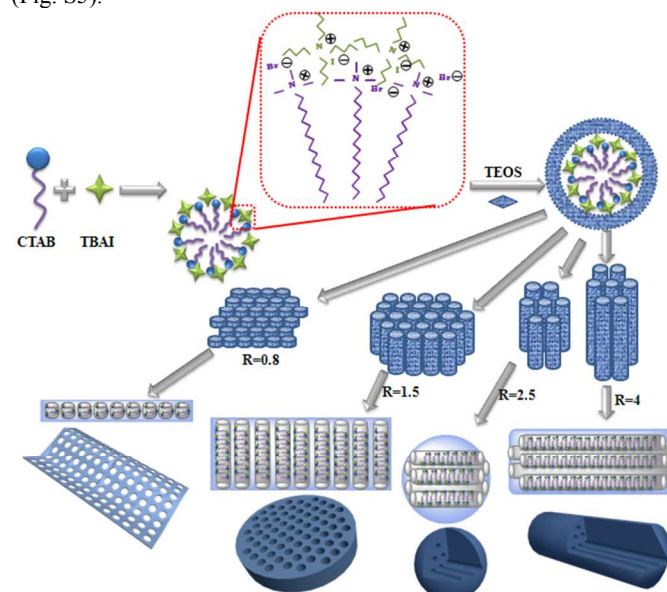


**Fig. 2** TEM images of (A) FMSN, (B) PMSN, (C) SMSN, and (D) RMSN after templates were removed.

MSNs of different shapes were synthesized following a simple protocol of ammonia-catalyzed condensation of tetraethyl orthosilicate (TEOS) using CTAB and TBAI as co-templates (see ESI for details). As revealed by the scanning electron micrographs (SEM) and transmission electron micrographs (TEM) in Fig. 1, by varying the mole ratio of CTAB to TBAI ( $R = [\text{CTAB}]/[\text{TBAI}]$ ), MSNs of different shapes were obtained. At  $R = 0.8$ , mesoporous silica films (FMSN) having an average thickness of 20 nm were formed (Fig. 1A). When  $R$  was changed to 1.5, the product turned into platelet-like nanostructure (PMSN) with an average particle size of  $\sim 5 \mu\text{m}$  and thickness of 100–300 nm (Fig. 1B). At  $R = 2.5$ , spheres (SMSN) with an average particle size of  $\sim 150 \text{ nm}$  were obtained (Fig. 1C). Further increasing of  $R$  to 4 led to rods (RMSN) having an average particle size of  $\sim 100 \text{ nm}$  in width and  $\sim 250 \text{ nm}$  in length (Fig. 1D). After removing the templates by solvent extraction in acidic ethanol, the pore channels could be clearly seen in these materials (Fig. 2). Nitrogen adsorption-desorption measurement of all four samples showed the typical type IV isotherm (Fig. S1, Table S1), which corresponded to ordered cylindrical mesostructures.<sup>19</sup> These materials possessed relatively high Brunauer-Emmet-Teller (BET) specific surface area and pore volume, ranging from 606 to 1121  $\text{m}^2/\text{g}$  and 0.48 to 1.03  $\text{cm}^3/\text{g}$ , respectively (Table S1). All four MSNs displayed a narrow pore size distribution, which centered around 2.8–3.4 nm as determined by the Barrett-Joyner-Halenda (BJH) method (Table S1).

A mechanism was proposed to account for the formation of these MSNs (Scheme 1). At the initial stage of the reaction, TBAI, being a smaller surfactant having a shorter chain length, could insert into the CTAB micelles to form self-assembled template structure.<sup>20</sup> This hypothesis is further supported by the results that the pore size increased with increasing mole ratio of TBAI to CTAB (Table S1). Ammonia-catalyzed hydrolysis of TEOS yielded negatively charged oligomeric silicate species that interact with CTAB/TBAI micelle surface through electrostatic interactions to form cylindrical CTAB/TBAI-silicate complex.<sup>21</sup> When  $R$  is around 0.8, the relatively higher concentration of TBAI is expected to decrease the critical micelle concentration (CMC),<sup>22</sup> which lead to a rapid aggregation of cylindrical micelles. The higher amount of TBAI also inhibited the growth of the micelles along the longitudinal axis, likely due to the reduced interactions of the CTAB alkyl tails caused by the diffusion of TBAI into the CTAB micelles.<sup>18a</sup> These led to thinner micelle aggregates, and when used as the template, gave film-like nanostructure with perpendicular mesoporous channels. Similar film structure was also obtained at  $R = 1.0$  (Fig. S2). When  $R$  was increased to 1.5, the increased CTAB concentration led to

continuous growth of micelles along the longitudinal direction of the cylindrical micelles. This type of template gave platelet-like nanostructure with mesoporous channels running along the thickness direction of PMSNs. Similar platelet structure was also obtained at  $R = 1.3$  (Fig. S3). At  $R = 2.5$  and 4, sphere- and rod-shaped nanostructures were obtained. These are similar to the MSNs synthesized by using CTAB alone, indicating that the role of TBAI was significantly weakened and the CTAB dominated the template structure. TBAI plays a significant role in the assembly of micelles. Without TBAI, spherical particles were formed (Fig. S4). However, TBAI alone as the template did not give any well-defined particles (Fig. S5).



**Scheme 1.** Proposed mechanism for the formation of MSNs of different shapes.

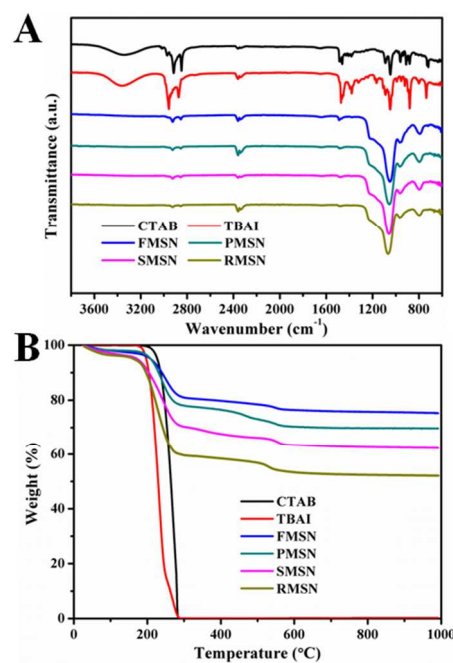


**Fig. 3** (A) FTIR spectra of CTAB, TBAI, and as-synthesized FMSN, PMSN, SMSN, and RMSN. (B) Thermal gravimetric analysis (TGA) curves of CTAB, TBAI, and as-synthesized FMSN, PMSN, SMSN, and RMSN.

Because these nanomaterials are synthesized under the same conditions, they provide an excellent platform to study the effect of shape on their biological performance. The as-synthesized MSNs contain quaternary ammonium halides, which allow us to use the antimicrobial activity as a tool to investigate the shape effect. Cationic surfactants are found in many household products, such as soaps, shampoos, detergents, and cosmetics. Their antibacterial activities could be attributed to: i) adsorption and penetration into the cell wall; ii) reaction with the cytoplasmic membrane followed by membrane disruption; iii) leakage of intracellular materials; iv) degradation of nucleic acids and proteins.<sup>23</sup> Halide ions can rapidly penetrate into microorganisms and cause bacteria death by attacking nucleotides, proteins, and fatty acids.<sup>23</sup> The as-synthesized different shaped MSNs with surfactants embedded inside displayed positive zeta potentials from +9.43 to +16.56 mV (Fig. S6), which allow them to capture the negative charged bacterial cells by electrostatic interaction (Fig. S7).<sup>24</sup> After surfactants were removed by extraction in acidic ethanol, the zeta potentials of the MSNs became negative (-34.89 to -19.39 mV, Fig. S8). The adsorption peaks in infrared spectroscopy at 2925  $\text{cm}^{-1}$  and 2847  $\text{cm}^{-1}$  suggest that CTAB and TBAI surfactants were embedded inside MSNs (Figs. 3A and S9). In the decomposition temperature range of CTAB and TBAI at 200-550  $^{\circ}\text{C}$ , weight loss of the as-synthesized MSNs was determined as 16%, 23%, 31%, and 40% for FMSN, PMSN, SMSN, and RMSN, respectively (Fig. 3B). This shows that the amount of surfactants entrapped was the lowest for the films, followed by platelets, spheres. Rods contained more than twice of the surfactants than the films.

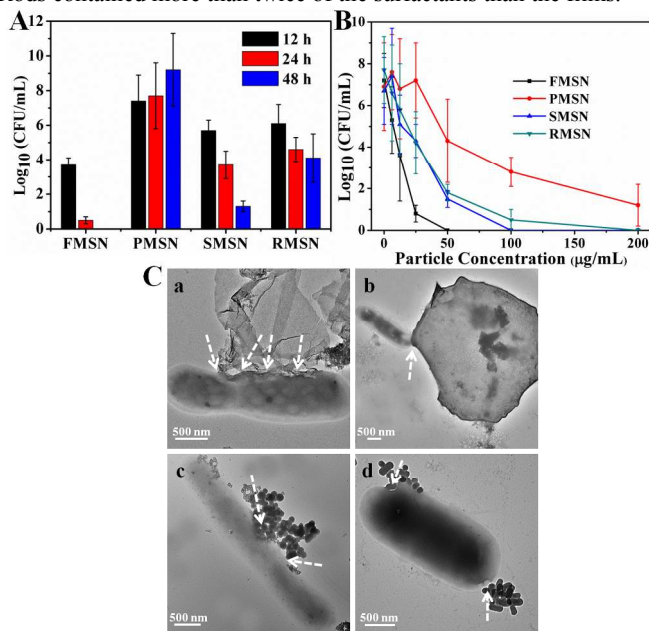


**Fig. 4** (A) Antibacterial activity of as-synthesized MSNs (25  $\mu\text{g}/\text{mL}$ ) against *M. smegmatis* strain mc<sup>2</sup> 651 for 12, 24, and 48 h. (B) Antibacterial activity of as-synthesized MSNs (particle concentration ranging from 0 to 200  $\mu\text{g}/\text{mL}$ ) against *M. smegmatis* strain mc<sup>2</sup> 651 for 24 h. (C) TEM images of FMSN (a), PMSN (b), SMSN (c), and RMSN (d) after incubated with bacteria for 4 h. Arrows show the interaction loci between bacteria and MSNs.

The antibacterial activity of as-synthesized MSNs was tested against mycobacteria (*M. smegmatis* strain mc<sup>2</sup> 651) at different particle concentration and incubation times. The minimal inhibitory concentration (MIC) of CTAB and TBAI was determined to be 18 and 90  $\mu\text{M}$ , respectively. The antibacterial activity of FMSN, PMSN, SMSN, and RMSN was measured by dilution plate counting at different incubation time (Fig. 4A) and particle concentration (Fig.

4B). The half inhibitory concentration ( $\text{IC}_{50}$ ) of mycobacteria treated by as-synthesized FMSN, PMSN, SMSN, and RMSN are 15, 93, 36, and 39  $\mu\text{g}/\text{mL}$ , respectively. The results showed that film exhibited the highest and platelet the lowest antibacterial activity. FMSN completely inhibited the formation of colonies at a low concentration of 25  $\mu\text{g}/\text{mL}$  after 48 h treatment. The release profiles of CTAB and TBAI from different shaped materials were further determined by suspending equal quantities of each materials in PBS (pH 7.4), and the amount of surfactants released were determined by comparing to standard calibration curves from bromide and iodide ion standard solutions (see Supporting Information). The results showed that the amount of released surfactants increased with time, and was highly dependent on particle shape. The films released the fastest, followed by rods and spheres, and finally platelets (Fig. S10). These results further supported that the antibacterial activity difference could be attributed to the shape-regulated release behavior of mesoporous silica materials.<sup>25</sup> The films have the shortest and vertical pore channels which enabled the fastest release of antibacterial agents.

The interactions between as-synthesized mesoporous materials and mycobacteria were further investigated under TEM. As is shown in Fig. 4C, as-synthesized MSNs bound to bacterial surface, likely due to the electrostatic attractions of surfactant-embedded MSNs with mycobacteria.<sup>24,26</sup> The direct interaction facilitated the release of CTAB and TBAI, and increased the local concentration of quaternary ammonium cations and halide ions. The film exhibited high binding to mycobacteria. In addition, the interactions between FMSN and mycobacteria occurred mostly at the film edges (Figs. 4C and S11). Similar observation has been reported for other film and 2D materials, where the edge-mediated interactions with cell membrane cause effective cell death.<sup>27</sup>

In summary, we developed a new and general strategy to synthesize MSNs of different shapes including film, platelet, sphere and rod simply by tuning the mole ratio of dual cationic surfactant templates CTAB and TBAI. The antibacterial activity of these as-synthesized MSNs against mycobacteria (*M. smegmatis* strain mc<sup>2</sup> 651) was shape-dependent. FMSNs exhibited the highest and fastest antibacterial activity than other particle shapes, albeit that the films contained the least amount of surfactants. Films also showed strong edge interactions with mycobacteria. Because these materials are synthesized using the same protocol, the results provide strong evidence for shape-dependent antimicrobial activities of nanomaterials.

The authors thank the financial support from the National Institutes of Health (R01GM080295, R21AI109896), and a startup grant from University of Massachusetts Lowell. We thank Professor William R. Jacobs of Albert Einstein College of Medicine for the kind gift of *M. smegmatis* strain mc<sup>2</sup> 651.

### Live subject statement

All bacteria handling and experimental protocols were performed in accordance with the University of Massachusetts Lowell guidelines. Procedures were conducted using approved Institutional Biosafety Committee (IBC) procedures (Registration No. 15-06-YAN).

### Notes and references

Department of Chemistry, University of Massachusetts, 1 University Ave., Lowell, MA 01854, USA. E-mail: mingdi\_yan@uml.edu; Fax: +1-978-934-3013; Tel: +1-978-934-3647

Electronic Supplementary Information (ESI) available: Experimental details, materials characterization and additional data. See DOI: 10.1039/c000000x/

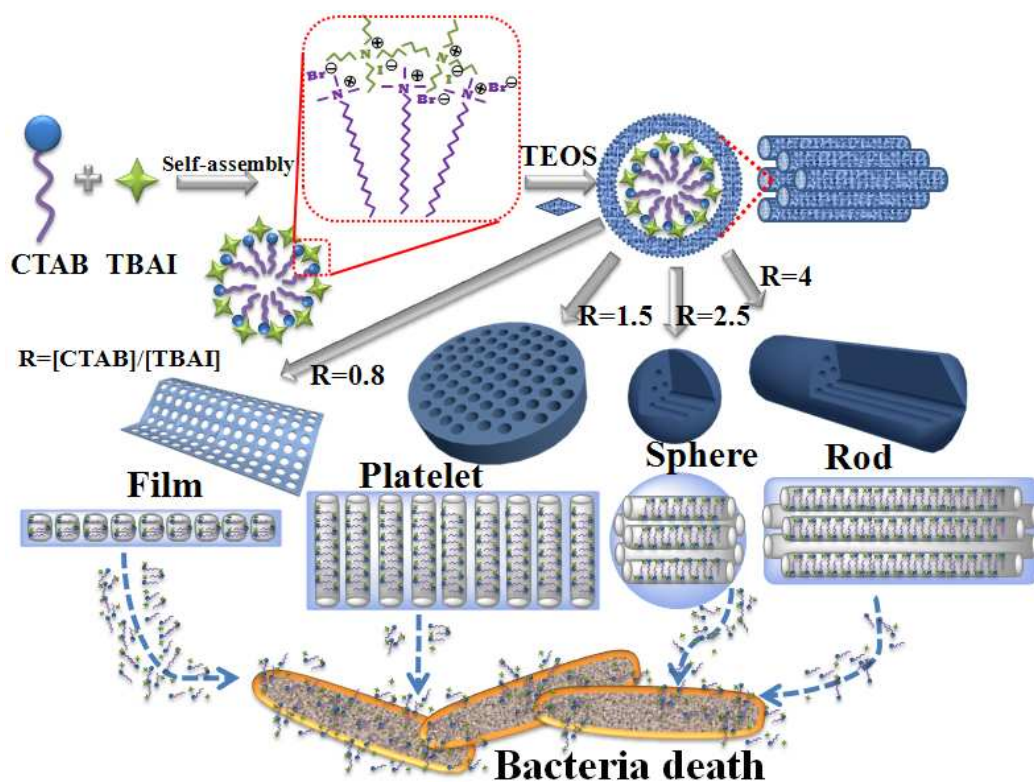
- 1 M. Colilla, B. González and M. Vallet-Regí, *Biomater. Sci.*, 2013, **1**, 114.
- 2 S. Hudson, J. Cooney and E. Magner, *Angew. Chem. Int. Ed.*, 2008, **47**, 8582.
- 3 J. A. Barreto, W. O'Malley, M. Kubeil, B. Graham, H. Stephan and L. Spiccia, *Adv. Mater.*, 2011, **23**, H18.
- 4 T. Yoshitomi and Y. Nagasaki, *Biomater. Sci.*, 2015, **3**, 810.
- 5 A. Stein, B. J. Melde and R. C. Schroden, *Adv. Mater.*, 2000, **12**, 1403.
- 6 J. Liu, S. Z. Qiao, J. S. Chen, X. W. Lou, X. R. Xing and G. Q. Lu, *Chem. Commun.*, 2011, **47**, 12578.
- 7 N. J. Hao, K. Neranon, O. Ramström and M. Yan, *Biosens. Bioelectron.*, doi:10.1016/j.bios.2015.07.031.
- 8 F. Hoffmann, M. Cornelius, J. Morell and M. Fröba, *Angew. Chem. Int. Ed.*, 2006, **45**, 3216.
- 9 (a) N. J. Hao, L. F. Li and F. Q. Tang, *J. Mater. Chem. A*, 2014, **2**, 11565; (b) K. Yang and Y. Q. Ma, *Nat. Nanotechnol.*, 2010, **5**, 579; (c) N. J. Hao, L. F. Li and F. Q. Tang, *J. Biomed. Nanotechnol.*, 2014, **10**, 2508.
- 10 (a) N. J. Hao, H. H. Yang, L. F. Li, L. L. Li and F. Q. Tang, *New J. Chem.*, 2014, **38**, 4258; (b) N. J. Hao, L. L. Li, Q. Zhang, X. L. Huang, X. W. Meng, Y. Q. Zhang, D. Chen, F. Q. Tang and L. F. Li, *Microporous Mesoporous Mater.*, 2012, **162**, 14; (c) G. Lelong, S. Bhattacharyya, S. Kline, T. Cacciaguerra, M. A. Gonzalez and M. L. Saboungi, *J. Phys. Chem. C*, 2008, **112**, 10674.
- 11 Q. Cai, Z. S. Luo, W. Q. Pang, Y. W. Fan, X. H. Chen and F. Z. Cui, *Chem. Mater.*, 2001, **10**, 258.
- 12 H. Jin, Z. Liu, T. Ohsuna, O. Terasaki, Y. Inoue, K. Sakamoto, T. Nakanishi, K. Ariga and S. Che, *Adv. Mater.*, 2006, **18**, 593.
- 13 H. M. Chen and J. H. He, *Chem. Commun.*, 2008, **44**, 4422.
- 14 D. Zhao, J. Sun, Q. Li and G. D. Stucky, *Chem. Mater.*, 2000, **12**, 275.
- 15 S. Huh, J. W. Wiench, J.-C. Yoo, M. Pruski and V. S.-Y. Lin, *Chem. Mater.*, 2003, **15**, 4247.
- 16 (a) K. J. Edler and B. Yang, *Chem. Soc. Rev.*, 2013, **42**, 3765; (b) N. Ehlert, P. P. Mueller, M. Stieve, T. Lenarz and P. Behrens, *Chem. Soc. Rev.*, 2013, **42**, 3847.
- 17 (a) B. C. Chen, H. P. Lin, M. C. Chao, C. Y. Mou and C. Y. Tang, *Adv. Mater.*, 2004, **16**, 1657; (b) Sujandi, S. E. Park, D. S. Han, S. C. Han, M. J. Jin and T. Ohsuna, *Chem. Commun.*, 2006, **42**, 4131.
- 18 (a) Z. G. Teng, G. F. Zheng, Y. Q. Dou, W. Li, C. Y. Mou, X. H. Zhang, A. M. Asiri and D. Y. Zhao, *Angew. Chem. Int. Ed.*, 2012, **51**, 2173; (b) A. Walcarius, E. Sibottier, M. Etienne and J. Ghanbaja, *Nat. Mater.*, 2007, **6**, 602.
- 19 K. S. W. Sing, D. H. Everett, R. A. W. Haul, L. Moscou, R. A. Pierotti, J. Rouquerol and T. Siemieniowska, *Pure Appl. Chem.*, 1985, **57**, 603.
- 20 P. L. He, B. Xu, H. L. Liu, S. He, F. Saleem and X. Wang, *Sci. Rep.*, 2013, **3**, 1833.
- 21 C. T. Kresge, M. E. Leonowicz, W. J. Roth, J. C. Vartuli and J. S. Beck, *Nature*, 1992, **359**, 710.
- 22 H. O. Pastore, M. Munsignatti, D. R. S. Bittencourt and M. M. Rippel, *Microporous Mesoporous Mater.*, 1999, **32**, 211.
- 23 G. McDonnell and A. D. Russell, *Clin. Microbio. Rev.*, 1999, **12**, 147.
- 24 N. J. Hao, K. W. Jayawardana, X. Chen and M. Yan, *ACS Appl. Mater. Interfaces*, 2015, **7**, 1040.
- 25 B. G. Trewyn, C. M. Whitman and V. S.-Y. Lin, *Nano Lett.*, 2004, **4**, 2139.
- 26 T. J. Kinnari, J. Esteban, E. Gomez-Barrena, N. Zamora, R. Fernandez-Roblas, A. Nieto, J. C. Doadrio, A. López-Noriega, E. Ruiz-Hernández, D. Arcos and M. Vallet-Regí, *J. Biomed. Mater. Res. A*, 2009, **89**, 215.
- 27 (a) Y. F. Li, H. Y. Yuan, A. von dem Bussche, M. Creighton, R. H. Hurt, A. B. Kane and H. J. Gao, *Proc. Natl. Acad. Sci. U.S.A.*, 2013, **110**, 12295; (b) Y. S. Tu, M. Lv, P. Xiu, T. Huynh, M. Zhang, M. Castelli, Z. R. Liu, Q. Huang, C. H. Fan, H. P. Fang and R. H. Zhou, *Nat. Nanotechnol.*, 2013, **8**, 594.

## Graphical abstract

## Shape Control of Mesoporous Silica Nanomaterials Templated with Dual Cationic Surfactants and Their Antibacterial Activities

Nanjing Hao, Xuan Chen, Kalana W. Jayawardana, Bin Wu, Madanodaya Sundhoro and Mingdi Yan\*

Department of Chemistry, University of Massachusetts, 1 University Ave., Lowell, MA 01854, USA. E-mail: mingdi\_yan@uml.edu; Fax: +1-978-934-3013; Tel: +1-978-934-3647



Mesoporous silica nanomaterials of different shape (film, platelet, sphere, rod) were synthesized by varying the mole ratio of dual surfactants. Shape-dependent antibacterial activity was observed.